

Properties of balanced flows with bottlenecks: Common stylized facts in finance and vibration-driven vehicles

G. A. Patterson^{1,*}, D. Sornette^{2,†} and D. R. Parisi^{1,‡}

¹*Instituto Tecnológico de Buenos Aires, CONICET, Lavardén 315, 1437 Ciudad Autónoma de Buenos Aires, Argentina*

²*Department of Management, Technology and Economics, ETH Zürich, 8092 Zürich, Switzerland;*

Institute of Risk Analysis, Prediction and Management, Academy for Advanced Interdisciplinary Studies,

Southern University of Science and Technology, Shenzhen 518055, China;

Tokyo Tech World Research Hub Initiative, Institute of Innovative Research, Tokyo Institute of Technology, Tokyo 152-8550, Japan;
and Swiss Finance Institute, University of Geneva, 1211 Geneva, Switzerland



(Received 9 July 2019; revised manuscript received 21 December 2019; accepted 16 March 2020; published 13 April 2020)

We study experimentally the properties of the flow of mechanical vibration-driven vehicles confined in two chambers connected through a narrow opening. We report that the density of particles around the opening presents critical behavior and scaling properties. By mapping this density to the financial market price, we document that the main stylized facts observed in financial systems have their counterparts in the mechanical system. The experimental model accurately reproduces financial properties such as scaling of the price fluctuation, volatility clustering, and multiscaling.

DOI: [10.1103/PhysRevE.101.042302](https://doi.org/10.1103/PhysRevE.101.042302)

I. INTRODUCTION

Financial stylized facts are robust statistical properties that are found in financial assets of different markets across time including stocks, portfolios, bond, and currencies [1,2]. Financial price fluctuations result from the flow of orders, where the dynamics of the buy and sell orders at a given time in the first layers [3] of the order book influence realized transactions. In this representation of a continuous flow of orders seen as particles populating the order book, a well-functioning market is one in which there is on average an approximate balance between buy and sell orders that occur in narrow price intervals near the best bid and the best ask. In contrast, when liquidity rarefies on the buy side and sell orders accumulate, large price changes and larger volatility can result, for instance, when a large market sell order occurs [4]. This picture of a flow of two types of buy and sell orders interacting in a narrow price interval suggests that a physical analog of almost balanced counterflows of particles could provide useful insights. A few proposals have already been made in this direction. For instance, Vamoş *et al.* presented the derivation of a one-dimensional hydrodynamic model to describe the stock price evolution [5]. Parisi *et al.* showed that a counterflow of simulated pedestrians through a door displays essentially all the stylized facts of financial markets, when mapping the density of agents around the opening to the logarithm of the market price [6]. Yura *et al.* established a remarkable quantitative analogy between the financial order book and a gas of creating and annihilating particles, which

provided a new physically based derivation of the geometric Brownian motion of financial prices [3,7]. In a similar vein, Bouchaud *et al.* noted that the volatility of financial markets is stabilized by a “liquidity molasses” created by the liquidity providers [8].

Previous studies have shown that agent-based models are capable of reproducing various stylized facts [9–11]. In the present work we report that a constrained system of self-propelled particles flowing through an opening exhibits critical behavior and scaling properties. Interestingly, we find that the emerging properties coincide with the so-called stylized facts of financial systems. Previous research investigated mechanical systems consisting of elongated vibration-driven vehicles (VDVs) confined to a specific geometry such as hopperlike constrictions [12], circular arenas [13], race-tracks [14], and parabolic traps [15].

Here we consider a geometry that is specifically designed to embody a balanced flow with a bottleneck, namely, two chambers connected by an opening. This particular geometry allows us to satisfy the following properties: competition between two opposite flows in the opening and constrictions that emerge from the interaction with the boundaries. While most numerical and experimental studies involve passive particles, we examine whether the analogy between financial price fluctuations and balanced flows with bottlenecks can be implemented experimentally by means of self-driven vehicles, which are more realistic analogs of market orders driven by purposeful traders. Our analysis of the temporal evolution of the density fluctuations of the VDV finds that they reproduce experimentally the main stylized facts of financial time series. This demonstrates that the proposed mechanical system presents statistical properties that are independent of their context, e.g., finance, physics, or engineering.

*gpatters@itba.edu.ar

†dsornette@ethz.ch

‡dparisi@itba.edu.ar

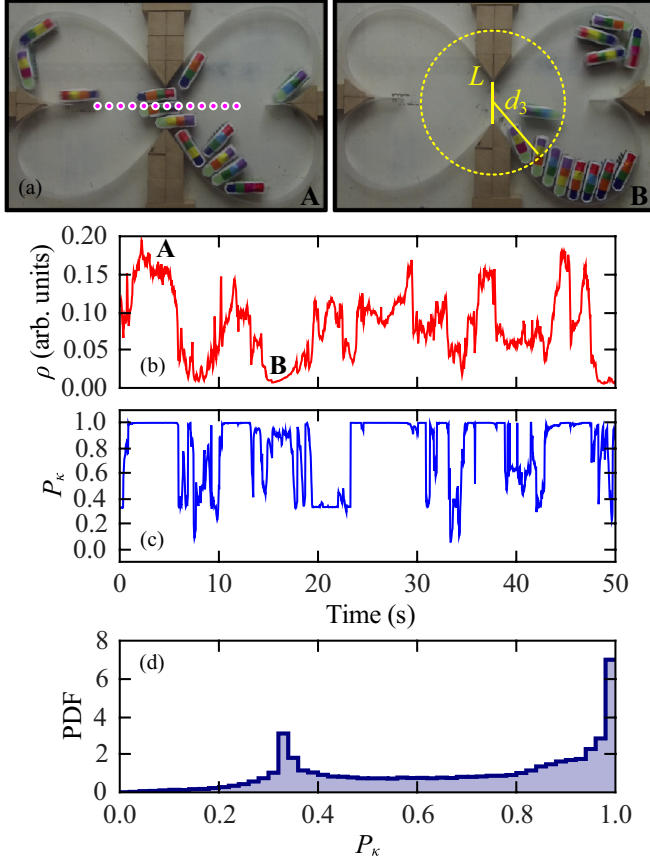


FIG. 1. (a) Snapshots of the VDV system. In panel B the distance d_3 is depicted. (b) Density time series of vibration-driven vehicles where A and B indicate the particular configurations shown in (a). (c) Time evolution of the polarization parameter P_κ . (d) Probability density function of P_κ .

II. EXPERIMENTAL SETUP

We used 13 vibration-driven vehicles commercially available as HEXBUG nano. The motion of these is originated by the vibration produced by an eccentric motor located inside the body. The motor is powered by a 1.5-V battery. The V DVs are standing on legs which resemble an asymmetric brush that rectifies the random vibration into a forward displacement. The direction of the V DVs is changed by the collision with other vehicles or with the boundaries of the arena. The dimensions of these are $43 \times 15 \times 18 \text{ mm}^3$. Each of them had a unique four-color label on it that allowed us to identify it univocally.

We built the closed geometry by connecting two chambers through an opening of size $L = 40 \text{ mm}$ as shown in Fig. 1(a). This particular design allowed us to generate a continuous flow of V DVs between both chambers. We used acetate tapes as flexible walls and wooden blocks (fixed to the floor) to set the opening size. A sheet of glass was placed on top, at a height of 19 mm, in order to prevent vehicles from overturning. We recorded the experiments with a GoPro Hero 3 camera placed on top of the arena and tracked the position of each agent with a time resolution $\tau = 1/29.97 \text{ s}$ given by the camera frame rate. We analyzed the first 10^5 frames of the experiment, that is, approximately 55 min.

III. RESULTS

As mentioned above, it is of interest to study the effect of constrictions on the dynamics of the system. For this we focused on the density around the opening estimated by the κ nearest neighbor. For this we determined the distance d_κ to the κ th nearest V DV from the center of the opening (x_0, y_0) as shown in panel B in Fig. 1(a). Finally, we estimated the density as

$$\rho \propto \frac{\kappa - 1}{d_\kappa^2}. \quad (1)$$

We studied the influence of different values of $\kappa = [2, 4]$ on the emerging statistical properties. While we found that the stylized facts are robustly present for these values, we choose to use $\kappa = 3$ because results better match the stylized facts of the financial markets (see Appendix A). Figure 1(b) shows the time evolution of ρ in a particular window of 50 s. Capital letters link the density values with the snapshots shown in Fig. 1(a).

We proceed to study different statistical properties that emerge from the mechanical system and compare them to the corresponding stylized facts from the Bitcoin cryptocurrency expressed in US dollars (BTCUSD) at a 1-h sampling rate [16]. Specifically, we take into account data ranging from 31 December 2012 to 30 June 2018. We consider the density ρ defined by the expression (1) as well as the logarithm of the price of BTCUSD, referring to their variation as the return

$$R_Y(t_i, j) = Y(t_{i+j}) - Y(t_i), \quad (2)$$

where t_i are the discrete time steps, j is the number of time steps over which the return is computed, and $Y(t_i)$ can be ρ for either the mechanism system or the logarithmic price of BTCUSD. We use $j = 1$ unless otherwise indicated. In analogy with the standardized return, we compute the standardized absolute return as

$$|R_Y^*(t_i, j)| = \frac{|R_Y(t_i, j)|}{\left(\sum_{h=1}^{N_T-j} |R_Y(t_h)|\right)/(N_T - j)}, \quad (3)$$

where $|R_Y|$ is the absolute value of the return and N_T is the total number of data points in the time series.

Because of their particular shape and their interaction with the boundaries, the V DVs tend to align with each other. This kind of emergent behavior for elongated particles was studied in [13,17]. In order to characterize the behavior of V DVs near the opening, we define a polarization parameter that is calculated from the orientations of the κ particles closest to the opening as

$$P_\kappa(t_i) = \frac{1}{\kappa} \left| \sum_{k=1}^{\kappa} \vec{e}_k(t_i) \right|, \quad (4)$$

where $\vec{e}_k(t_i)$ is the direction of the particle k at time t_i . Figure 1(c) shows the time evolution of the polarization while Fig. 1(d) shows the probability density function (PDF) computed over all t_i . The results exhibit two maxima that

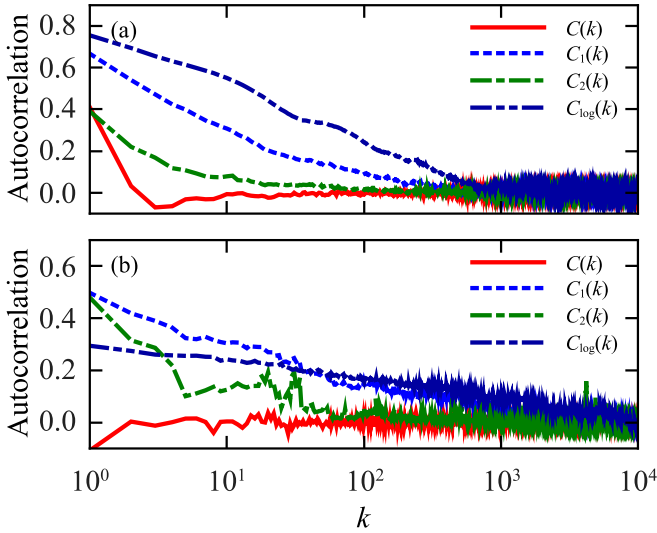


FIG. 2. Autocorrelation function of the (a) VDV and (b) BTCUSD returns (red solid line), absolute returns (royal blue short-dashed line), square returns (green long-dash–short-dashed line), and logarithm of absolute returns (navy blue long-dash–double-short-dashed line).

correspond to configurations of parallel and antiparallel alignment. These findings show that those particles that are closer to the opening evolve between disordered motion and herding. It can be observed that the system operates in a metastable state in which saturated high polarization values alternate with low polarization values. A similar phenomenon was found in the simulated pedestrian system [6] for an optimum value of the individualistic parameter. This evidences that the stylized facts emerge when the systems defined as balanced flows with bottlenecks operate near a critical state.

A. Correlation of returns and volatility clustering

We now examine several statistical properties of the returns. The sample correlation function of the returns is defined as

$$C(k) = \text{corr}(R_Y(t_i + k\tau), R_Y(t_i)), \quad (5)$$

where k is the time lag and τ is the time resolution. Figure 2(a) shows the estimated autocorrelation for $Y = \rho$ as a function of the time lag k , revealing that there is an absence of linear autocorrelation for times larger than ten lags. Similar results are obtained for Y equal to the logarithmic price of BTCUSD, shown in Fig. 2(b).

This fast decay of the correlation of returns should be contrasted with the long memory exhibited by the autocorrelation function of the absolute returns, associated with volatility clustering. To quantify this phenomenon, we follow standard procedures and estimate the autocorrelation function of an arbitrary power α of the absolute returns defined as

$$C_\alpha(k) = \text{corr}(|R_Y(t_i + k\tau)|^\alpha, |R_Y(t_i)|^\alpha). \quad (6)$$

The $C_1(k)$ and $C_2(k)$ are shown for $Y = \rho$ in Fig. 2(a) and for Y equal to the logarithmic price of BTCUSD in Fig. 2(b). This result is compatible with other observations in financial systems [18,19], which document a power-law decay $C_\alpha(k) \propto$

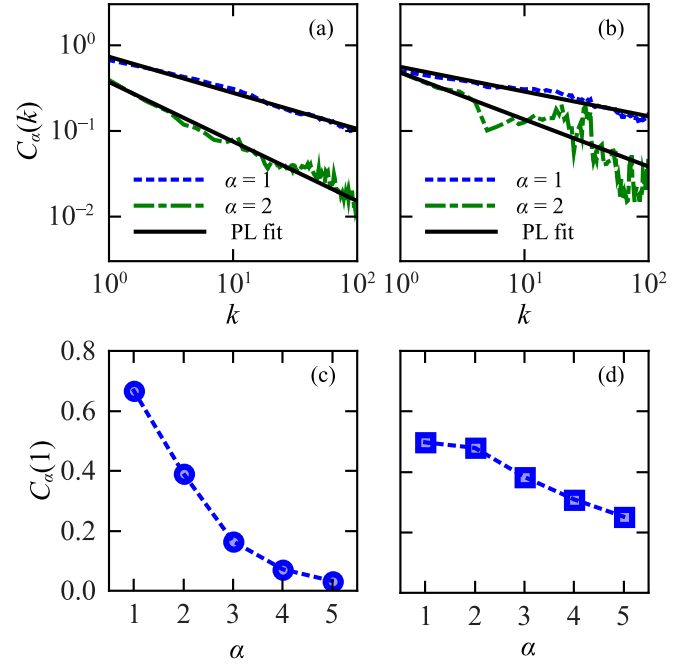


FIG. 3. Autocorrelation function of the absolute (blue short-dashed line) and squared returns (green long-dash–short-dashed line) for the (a) VDV and (b) BTCUSD systems. Black solid lines stand for PL fits. Also shown is the first lag of the autocorrelation for different exponents α for the (c) VDV and (d) BTCUSD systems.

$k^{-\beta(\alpha)}$. Figures 3(a) and 3(b) show the autocorrelation of the absolute returns for powers $\alpha = 1$ and 2 for the VDV and BTCUSD systems, respectively. We fit power-law functions using the least-squares method and our calibration yields $\beta(1) = 0.4$ and $\beta(2) = 0.6$ for the VDV system and $\beta(1) = 0.3$ and $\beta(2) = 0.55$ for the logarithmic price of BTCUSD. The closeness of these exponents for the VDV system and logarithmic price of BTCUSD is a quite remarkable substantiation of the analogy between the two systems. Moreover, as stated by Ding and Granger for financial systems [20], we have verified that the autocorrelation for a given time lag k reaches its maximum at $\alpha = 1$ for both systems as can be seen in Figs. 3(c) and 3(d). Motivated by multifractal stochastic volatility models [21,22], we also estimated the autocorrelations of the logarithm of the absolute returns

$$C_{\log}(k) = \text{corr}(\log |R_Y(t_i + k\tau)|, \log |R_Y(t_i)|), \quad (7)$$

which are shown in Fig. 2. One can observe a quasilinear decay $C_{\log}(k)$ as a function of $\ln k$ up to an integral timescale approximately equal to $k_T \simeq 10^3$ for the VDV system and $k_T \simeq 10^4$ for the logarithmic price of BTCUSD. In both cases, the integral timescales are much larger than that found for the autocorrelation of $|R_Y|$. These results are in agreement with the postulated form proposed by Muzy *et al.* [21].

This slow decay of the autocorrelation of the absolute values of returns for the VDV cannot be associated, as in financial systems, with the existence of an explicit decision mechanism and competition between strategies. However, we note that decisions could be replaced by the more complex particle geometry (anisotropic), in contrast with the isotropic disk geometry in computer simulations [6]. The elongated form,

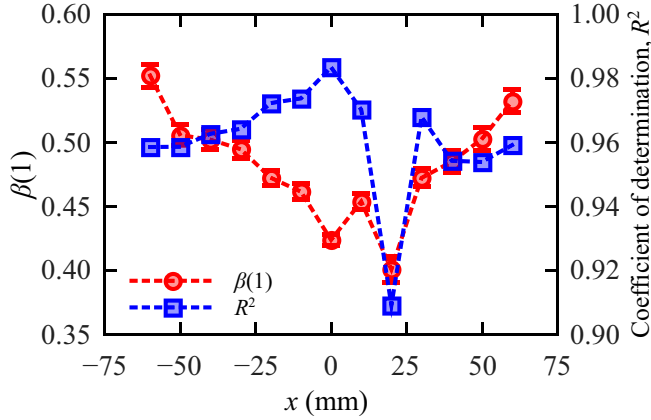


FIG. 4. Power-law exponents and coefficient of determination obtained from fits of the autocorrelation of the absolute values of density when estimated at different measurement points.

along with the vibration mechanism, can produce changes of direction when interacting near the door, which change the “state” of the particle, i.e., the direction of particle motions. This is connected with the system operating in metastable states so that the polarization alternates between two distinctive types of order as shown in Fig. 1.

Additionally, we have studied the influence of the opening on the evolution of the system. For this, we estimated the local density of particles for the measurement points shown in Fig. 1(a). Then, for each time series, we computed the autocorrelation of the absolute returns and fitted a power-law (PL) function as in Fig. 3. The obtained exponents $\beta(1)$ are shown in Fig. 4 with the related coefficient of determination R^2 . Data reveal that the better approximation (largest R^2) is found for the density estimated at the center of the opening. For this series, we found that the density measured around the opening presents the longest correlation decay, namely, a low value of $\beta(1)$. As the measurement point moves away from the center, the absolute values of density are less correlated, that is, $\beta(1)$ increases. These results show that the volatility clustering, one of the main stylized facts, is maximized at the center of the opening.

B. Fat tails and aggregational Gaussianity

Another stylized fact is the non-Gaussian and fat-tailed nature of the probability density function of returns [22–24]. Figure 5 shows the complementary cumulative distribution function (CCDF) of $|R_Y^*|$ for $Y = \rho$ [Fig. 5(a)] and Y equal to the logarithmic price of BTCUSD [Fig. 5(b)] for returns estimated on $j = 1, 100,$ and 500 time steps. The CCDFs of returns exhibit fatter tails than Gaussian distributions, while at the same time they converge to Gaussian distributions under time aggregation, as can be seen from their change from $j = 1$ to 100 and to 500 [25]. In Appendix B we present quantitative results regarding the fitting of the distributions.

C. Scaling of distribution maxima

The properties of the central part of the distribution, that is, the probability of zero returns, constitute another stylized fact previously reported for financial returns. We thus estimate

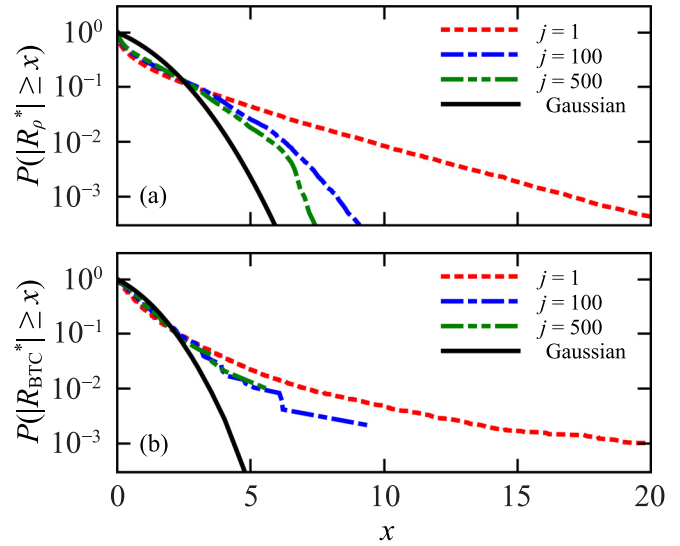


FIG. 5. Complementary cumulative distribution function for the standardized absolute returns of the (a) VDV and (b) BTCUSD systems computed at different time steps j . The solid line stands for the CCDF of the nearest Gaussian distribution.

the dependence of the maximum $P(R_Y = 0)$ of the distribution of returns for various time steps j using a probability density estimator based on a normal kernel function. As expected, we find that $P(R_Y = 0)$ decays according to a power law $P(R_\rho = 0) \propto j^{-\delta}$, with $\delta = 0.81$ for the VDV system and $\delta = 0.59$ for BTCUSD as shown in Fig. 6. Fitting was done using the least-squares method. These results are in accordance with, for instance, those obtained for the S&P500 index [26].

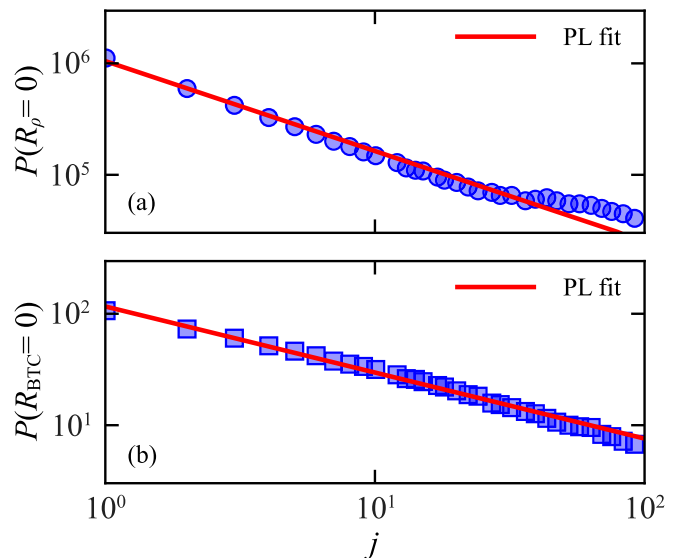


FIG. 6. Probability of zero return as a function of time step j for the (a) VDV and (b) BTCUSD systems. The exponents of the power-law fits are $\delta = 0.81$ for the VDV system and $\delta = 0.59$ for BTCUSD system.

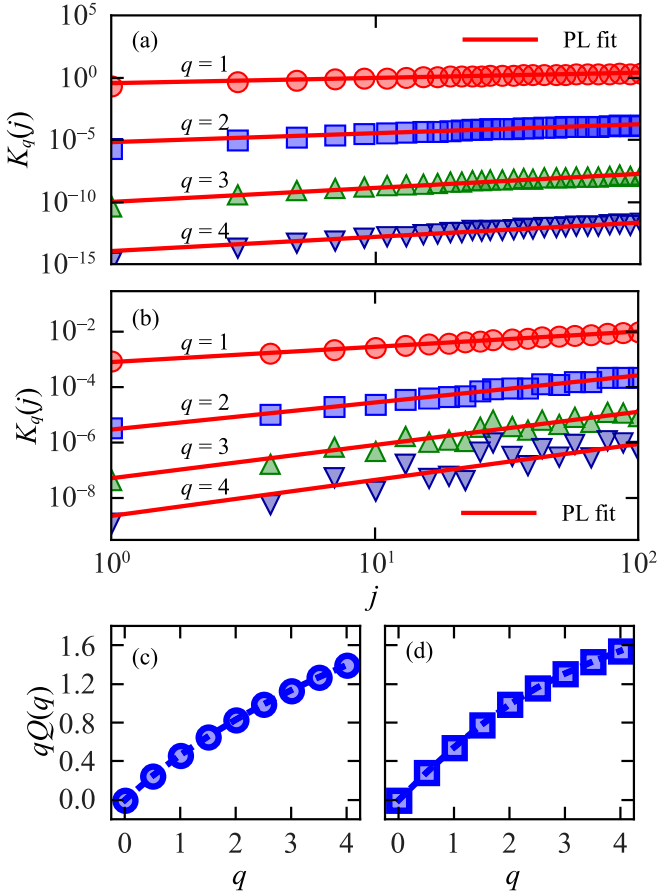


FIG. 7. (a) Plot of $K_q(j)$ of R_ρ as a function of time step j for $q = 1, 2, 3$, and 4 . Solid lines show the PL fits. (b) Plot of $K_q(j)$ and PL fits for the BTCUSD system. (c) Exponents $qQ(q)$ as a function of q for the VDV system, showing a nonlinear relationship. (d) The $qQ(q)$ function for the BTCUSD system.

D. Multifractality

Next we perform a multifractal analysis to verify the scaling property of the moments [27–29]

$$K_q(j) = \langle |R_Y(t_i, j)|^q \rangle \propto j^{qQ(q)}, \quad (8)$$

where the operator $\langle \cdot \rangle$ is the time average over all t_i and q is the order of the moment. Figures 7(a) and 7(b) show $K_q(j)$ as a function of j for the VDV and BTCUSD systems, respectively. The power-law scaling $K_q(j) \propto j^{qQ(q)}$ is confirmed, with exponents $qQ(q)$ that are nonlinear functions of q qualifying the presence of multifractality [27,30] as seen in Figs. 7(c) and 7(d) for the VDV and BTCUSD systems, respectively. The exponents are obtained using least-squares calibration. These results are in accordance with the BTCUSD multifractal analysis shown in Refs. [31,32].

E. Hurst exponent

The last property that we analyze is the long-range dependence of the time series of absolute returns $|R_\rho|$, which we investigate by means of the detrended fluctuation analysis [33–35]. Following this approach, we compute the root-mean-square fluctuation of the integrated and detrended time

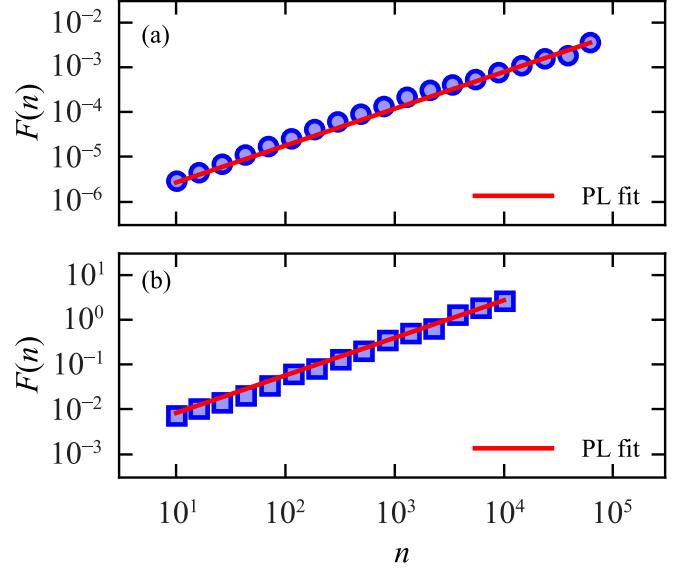


FIG. 8. Detrended fluctuation analysis for the (a) VDV and (b) BTCUSD systems. Solid lines stand for PL fits.

series $F(n)$ and plotted against n as shown in Fig. 8 for the VDV system [Fig. 8(a)] and the BTCUSD system [Fig. 8(b)]. In both we find a linear relationship on a log-log scale that leads us to fit a PL function. Our estimation of the Hurst exponent gives $H = 0.82$ for the VDV system [Fig. 8(a)]. This value indicates that the VDV system presents significant persistence. For the BTCUSD system [Fig. 8(b)], we find an almost identical value $H = 0.83$. These results indicate that periods with positive trends tend to be followed by periods with similar trends.

F. Mechanical-financial equivalence equation

Finally, we further motivate the proposed analogy between the mechanical system of VDV and financial price fluctuations by presenting the equation for the rate of change of the density in the self-propelled particle system as

$$\frac{\partial \rho}{\partial t} = -2 \frac{\rho}{r_\kappa} [\dot{r}_\kappa] + \epsilon, \quad (9)$$

where r_κ is the radial component of the position of the κ th particle from the center of the constriction (used to compute the density ρ), \dot{r}_κ is the radial velocity, and ϵ represents velocity fluctuations stemming mainly from the interchanges of other particles with the κ th particle. This equation can be further mapped onto the price evolution equation in finance

$$\frac{dP}{dt} = \frac{D - S}{W}, \quad (10)$$

where P is the price, D the demand, S the supply, and W the market depth. The derivation is demonstrated as follows. First, we write $\frac{\partial \rho}{\partial t}$ for our mechanical system. We choose to calculate the density in a nonparametric way, by fixing the number of particles and measuring the area that contains them, $\rho(r_\kappa, t) = \frac{\kappa-1}{\pi r_\kappa^2(t)}$, where $r_\kappa(t)$ is the radial position of the κ th

particle from the center of the constriction. Thus,

$$\frac{\partial \rho}{\partial t} = \frac{\partial[(\kappa - 1)/(\pi r_\kappa^2(t))]}{\partial t} = -2[(\kappa - 1)/\pi] \frac{\dot{r}_\kappa}{r_\kappa^3}. \quad (11)$$

Considering the definition of the density we can write

$$\frac{\partial \rho}{\partial t} = -2 \frac{\rho}{r_\kappa} \dot{r}_\kappa. \quad (12)$$

Now we consider that our mechanical system provides at least two kind of fluctuations for the velocity of the κ th particle. One corresponds to the high frequency due to the vibration mechanism that propels the VDV's. The second source of fluctuation appears when particle $\kappa - 1$ or $\kappa + 1$ interchanges places and becomes particle κ . This change of particles may occur at different radial velocities and thus it produces a discontinuity on it. So these sources of velocity fluctuations are expressed by writing the radial velocity as its mean value over time plus a fluctuation term: $\dot{r}_\kappa = \langle \dot{r}_\kappa \rangle + \epsilon$. With this, Eq. (12) becomes

$$\frac{\partial \rho(r_\kappa, t)}{\partial t} = -2 \frac{\rho}{r_\kappa} [\langle \dot{r}_\kappa \rangle + \epsilon]. \quad (13)$$

Defining a virtual flow of particles as $J = -\rho \dot{r}$, we can write Eq. (13) as

$$\frac{\partial \rho(r_\kappa, t)}{\partial t} = -\frac{\partial J}{\partial r_\kappa} + s(r_\kappa, t), \quad (14)$$

where $s(r_\kappa, t)$ is a source term of flowing particles related to the fluctuation velocity term ϵ .

Equation (14) is analogous to the one corresponding to price dynamics in the order book if we take it along the price axis, where $\rho(p, t)$ is the density of orders at a given price p at time t ; $J(p, t)$ is correspondingly the flux of orders at price p at time t in the order book. In this case, the equation reads

$$\frac{\partial \rho(p, t)}{\partial t} = -\frac{\partial J}{\partial p} + s(p, t). \quad (15)$$

This representation corresponds to the microscopic level of the order book, as described in [3,7]. In particular, it provides a microscopic origin of the random-walk nature of prices with a physical picture analogous to the Brownian motion [3]. Specifically, it maps the financial price dynamics to that of a micron-sized particle in a solvent undergoing a random walk in space. In other words, $\rho(p, t)$ can be visualized as the density of particles at position p at time t . These particles move around, are created when a new order occurs, and are annihilated when an order is removed or executed when a trade is made. This last phenomenon is taken into account by the source and sink terms of Eq. (15).

The observed price $P(t)$ can be approximated at a coarse-grained level as the center of gravity of the set of prices along the order book axis. Thus, $P(t)$ is defined as

$$P(t) = \int dp p \rho(p, t). \quad (16)$$

Then

$$\frac{dP}{dt} = \int dp p \partial \rho(p, t) / \partial t \quad (17)$$

and

$$\frac{dP}{dt} = - \int dp p \partial J(p, t) / \partial p + \int dp p s(p, t). \quad (18)$$

Integrating by parts, we obtain that (assuming vanishing flux and its derivative at $+$ and $-$ infinity)

$$\frac{dP}{dt} = \int dp J(p, t) + \int dp p s(p, t). \quad (19)$$

In the simplest model, $J \propto -\partial \rho(p, t) / \partial p$ expresses a tendency for orders to equilibrate. Then the first integral in Eq. (19) vanishes and we are left with

$$\frac{dP}{dt} = \int dp p s(p, t). \quad (20)$$

Now it is necessary to differentiate between the ask $[\rho_+(p, t)]$ and bid $[\rho_-(p, t)]$ side of the order book. The former is expressed as

$$\frac{\partial \rho_+(p, t)}{\partial t} = -\frac{\partial J}{\partial p} + s_+(p, t), \quad (21)$$

while the latter is

$$\frac{\partial \rho_-(p, t)}{\partial t} = -\frac{\partial J}{\partial p} + s_-(p, t). \quad (22)$$

In this way, the price equation becomes

$$P(t) = \frac{1}{W} \int dp p [\rho_-(p, t) + \rho_+(p, t)]. \quad (23)$$

This is the key equation capturing the phenomenon of the price dynamics as a balance between the bid and ask prices along the order book. We introduce a proportionality constant $1/W$ to express that the price is proportional to the overall unbalance between all the orders in the order book.

Following the same steps as from Eq. (17) to Eq. (20), we find that

$$\frac{dP}{dt} = \frac{1}{W} \int dp p [s_-(p, t) - s_+(p, t)]. \quad (24)$$

By definition, demand $D = \int dp p s_-(p, t)$ and supply $S = \int dp p s_+(p, t)$ and we obtain

$$\frac{dP}{dt} = \frac{D - S}{W}. \quad (25)$$

IV. CONCLUSION

In summary, we have studied the properties of the flow of mechanical self-propelled particles confined in a geometry described by two chambers that connect through a narrow opening. While the system configuration produces a continuous flow of particles between the two chambers, their elongated geometry leads to transient spatial clustering and coherent orientation, akin to a herding process in finance. By defining the polarization parameter, we observed that the three nearest particles from the center of the opening exhibit strong transitory alignments. Further, we found that the vibration-driven vehicle system exhibits critical behavior and scaling properties in agreement with the so-called stylized facts ob-

served in financial systems. We illustrated this by comparing with similar properties of the financial returns of the Bitcoin price series expressed in US dollars. We found excellent agreement between these two systems in the sense that they share the following facts: fast decay of the autocorrelation of returns; slow decay of the autocorrelation of absolute returns, of their square, and of the logarithm of absolute returns; fat tails of the distribution of returns; aggregational Gaussianity; scaling of the probability of zero return; multifractality; and self-similarity with persistence quantified by a large value of the Hurst exponent.

Therefore, the VDV system, which is ruled by simple repulsion and friction interactions, exhibits essentially the most important statistical properties shown by a system as complex as that of financial markets. By comparing the experimental VDV system with the numerical results of simulated pedestrians [6], we hypothesized what seems to be the key ingredients: (i) two groups of interacting agents flowing in counterflow configuration, which is the analog in finance to the buyers and sellers initiating trades; (ii) a geometrical constriction that funnels the flow, which is the analog in finance to the narrow price interval close to the bid-ask spread around which transactions are executed [36,37]; and (iii) the continuity equation for the flow [Eq. (9)], which has a counterpart in financial systems [Eq. (10)].

We can also identify a number of characteristics from the simulated [6] and experimental physical systems that are irrelevant for the emergence of the stylized facts: (a) the particular geometries of the connected chambers, which are square for the simulated particles and heart-shaped here; (b) periodic boundary conditions in the simulation that are not present in the experiment; (c) the shape of the particle (isotropic vs elongated); (d) the specific form of the interactions between particles; (e) the specific propulsion mechanism of the particles; (f) the decision-making capacity of the simulated pedestrians are replaced by the complex shape and alignment process in the experimental counterpart; and (g) the model approximations and numerical simplifications are not present in the experiment. Because of these important differences, we can state that the simulated and experimental systems are two different systems sharing only the key ingredients defined above. This enhances the evidence suggesting that these ingredients, also shared by the financial systems, are at the basis of the mechanisms from which the stylized facts emerge.

ACKNOWLEDGMENTS

This work was funded by Project No. ITBACyT-33 [Instituto Tecnológico de Buenos Aires (ITBA)] and Grant No. PID2015-003 (Agencia Nacional de Promoción Científica y Tecnológica, ITBA, and Urbix Technologies S.A., Argentina). D.R.P. is grateful to Román y Matilda for their help with the first prototype of the experiment. G.A.P. is grateful to Gonzalo Nardini, María Eugenia Sakuda, and Diego Vázquez for their help with the tracking system.

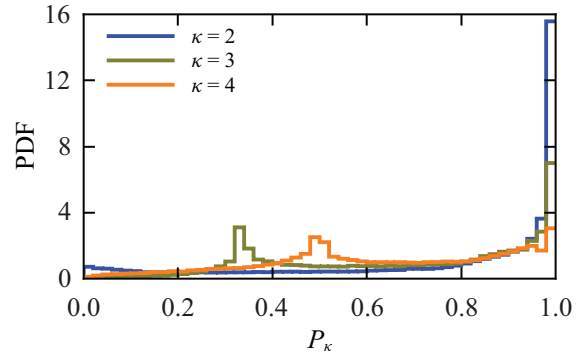


FIG. 9. Comparison between the PDF of P_κ for $\kappa = [2, 4]$.

APPENDIX A

We study how κ affects the PDF of the polarization. For this we take $\kappa \in [2, 4]$ and find that the corresponding distributions are bimodal, as shown in Fig. 9. In the case of $\kappa = 2$, there is a dominant maximum reflecting a greater probability of finding the two V DVs in parallel alignment ($P_\kappa \approx 1$). In contrast, there is a small probability of finding the two V DVs in antiparallel alignment ($P_\kappa \approx 0$). For $\kappa = 4$, as in the case of $\kappa = 3$, the peak heights of the distributions are more similar, showing a parity between antiparallel and parallel configurations.

We choose to show results using $\kappa = 3$ because one important stylized fact is more pronounced, as is the case of the

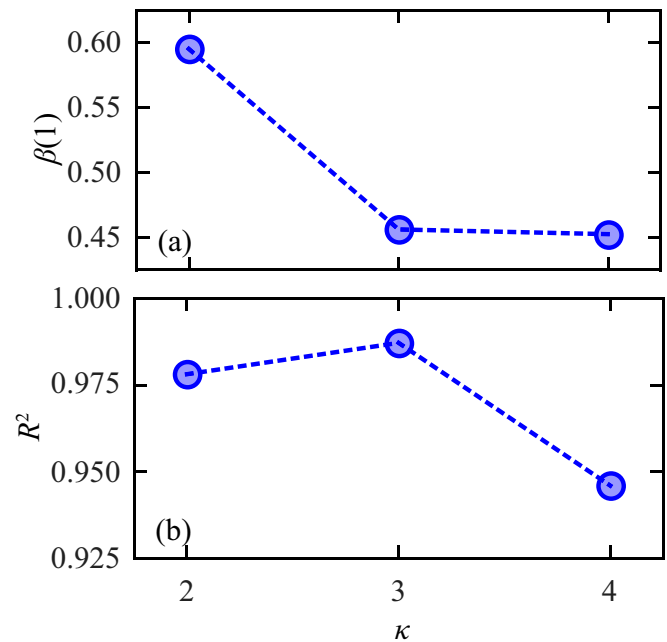


FIG. 10. (a) Decay of the autocorrelation of $|R_\rho|$ as a function of κ . (b) Coefficient of determination obtained from the fitting procedure.

power-law decay of the autocorrelation of absolute returns. For $\kappa = [2, 4]$ we find that $\beta(1)$ ranges from 0.4 to 0.6 but the coefficient of determination R^2 is maximized for $\kappa = 3$ as can be seen in Figs. 10(a) and 10(b), respectively.

APPENDIX B

Figure 11(a) shows results for $j = 1$, where we find that the CCDF corresponding to the VDV system is well described by a stretched exponential distribution with exponent 0.71 similar to that reported in other financial systems [23,24,38]. For the BTCUSD system [Fig. 11(b)], the CCDF of the returns of the logarithmic price of BTCUSD is better fitted by a power law with exponent 3.3.

For the case of BTCUSD, we follow the procedure introduced by Clauset *et al.* [39] to find the power-law exponent and the threshold value above which the fit is valid. In the case of the VDV system, we find that the data are compatible with a Weibull distribution. Then we follow an *ad hoc* maximum likelihood estimation procedure to estimate the parameters.

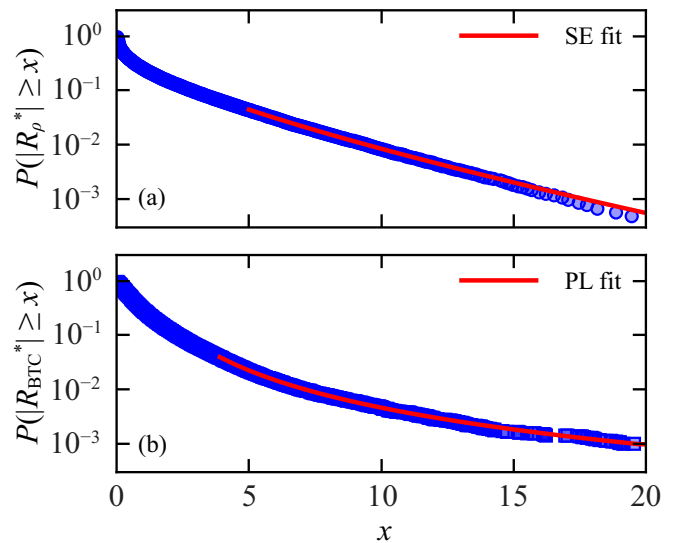


FIG. 11. (a) Complementary cumulative distribution function for the VDV returns. The solid line stands for SE fit. (b) The CCDF for BTCUSD returns and the corresponding PL fit shown by the solid line.

- [1] R. N. Mantegna and H. E. Stanley, *Introduction to Econophysics: Correlations and Complexity in Finance* (Cambridge University Press, Cambridge, 1999).
- [2] J. L. McCauley, *Dynamics of Markets: The New Financial Economics* (Cambridge University Press, Cambridge, 2009).
- [3] Y. Yura, H. Takayasu, D. Sornette, and M. Takayasu, *Phys. Rev. Lett.* **112**, 098703 (2014).
- [4] T. Sueshige, D. Sornette, H. Takayasu, and M. Takayasu, *PLoS One* **14**, e0220645 (2019).
- [5] C. Vamoş, N. Suciuc, and W. Blaj, *Physica A* **287**, 461 (2000).
- [6] D. R. Parisi, D. Sornette, and D. Helbing, *Phys. Rev. E* **87**, 012804 (2013).
- [7] Y. Yura, H. Takayasu, D. Sornette, and M. Takayasu, *Phys. Rev. E* **92**, 042811 (2015).
- [8] J.-P. Bouchaud, J. Kockelkoren, and M. Potters, *Quant. Financ.* **6**, 115 (2006).
- [9] G. Iori, *J. Econ. Behav. Organ.* **49**, 269 (2002).
- [10] T. Takaishi, *Int. J. Mod. Phys. C* **16**, 1311 (2005).
- [11] S. V. Vikram and S. Sinha, *Phys. Rev. E* **83**, 016101 (2011).
- [12] G. A. Patterson, P. I. Fierens, F. Sanguiliano Jimka, P. G. König, A. Garcimartín, I. Zuriguel, L. A. Pugnaroni, and D. R. Parisi, *Phys. Rev. Lett.* **119**, 248301 (2017).
- [13] A. Deblais, T. Barois, T. Guerin, P. H. Delville, R. Vaudaine, J. S. Lintuvuori, J. F. Boudet, J. C. Baret, and H. Kellay, *Phys. Rev. Lett.* **120**, 188002 (2018).
- [14] T. Barois, J.-F. Boudet, N. Lanchon, J. S. Lintuvuori, and H. Kellay, *Phys. Rev. E* **99**, 052605 (2019).
- [15] O. Dauchot and V. Démery, *Phys. Rev. Lett.* **122**, 068002 (2019).
- [16] Bitcoincharts, <https://bitcoincharts.com/charts>.
- [17] A. Baskaran and M. C. Marchetti, *Phys. Rev. Lett.* **101**, 268101 (2008).
- [18] R. Cont, M. Potters, and J.-P. Bouchaud, in *Scale Invariance and Beyond*, edited by B. Dubrulle, F. Graner, and D. Sornette (Springer, Berlin, 1997), pp. 75–85.
- [19] Z. Ding, C. W. J. Granger, and R. F. Engle, *Essays in Econometrics: Collected Papers of Clive W. J. Granger* (Harvard University Press, USA, 1993), pp. 349–372.
- [20] Z. Ding and C. W. Granger, *J. Econometrics* **73**, 185 (1996).
- [21] J. Muzy, J. Delour, and E. Bacry, *Eur. Phys. J. B* **17**, 537 (2000).
- [22] R. Cont, *Quant. Financ.* **1**, 223 (2001).
- [23] Y. Malevergne and D. Sornette, *Quant. Financ.* **4**, 17 (2004).
- [24] Y. Malevergne, V. Pisarenko, and D. Sornette, *Quant. Financ.* **5**, 379 (2005).
- [25] J.-P. Bouchaud and M. Potters, *Theory of Financial Risk and Derivative Pricing: From Statistical Physics to Risk Management* (Cambridge University Press, Cambridge, 2003).
- [26] R. N. Mantegna and H. E. Stanley, *Nature (London)* **376**, 46 (1995).
- [27] T. Di Matteo, *Quant. Financ.* **7**, 21 (2007).
- [28] T. Aste and T. Di Matteo, in *Complex Physical, Biophysical and Econophysical Systems*, edited by R. L. Dewar and F. Detering, World Scientific Lecture Notes in Complex Systems Vol. 9 (World Scientific, Singapore, 2010), pp. 1–35.
- [29] R. J. Buonocore, G. Brandi, R. N. Mantegna, and T. Di Matteo, *Quant. Financ.* **20**, 133 (2020).
- [30] Z.-Q. Jiang, W.-J. Xie, W.-X. Zhou, and D. Sornette, *Phys. Rep.* (2018), doi: 10.1088/1361-6633/ab42fb.
- [31] A. F. Bariviera, M. J. Basgall, W. Hasperu e, and M. Naiouf, *Physica A* **484**, 82 (2017).
- [32] S. Drozd, R. Gebarowski, L. Minati, P. Oswiecimka, and M. Watorek, *Chaos* **28**, 071101 (2018).
- [33] C.-K. Peng, S. V. Buldyrev, S. Havlin, M. Simons, H. E. Stanley, and A. L. Goldberger, *Phys. Rev. E* **49**, 1685 (1994).
- [34] C. Peng, S. Havlin, H. E. Stanley, and A. L. Goldberger, *Chaos* **5**, 82 (1995).

- [35] Y.-H. Shao, G.-F. Gu, Z.-Q. Jiang, W.-X. Zhou, and D. Sornette, [Sci. Rep. **2**, 835 \(2012\)](#).
- [36] B. Tóth, Y. Lempérière, C. Deremble, J. de Lataillade, J. Kockelkoren, and J.-P. Bouchaud, [Phys. Rev. X **1**, 021006 \(2011\)](#).
- [37] M. Schnaubelt, J. Rende, and C. Krauss, [J. Risk Financ. Manage. **12**, 25 \(2019\)](#).
- [38] J. Laherrère and D. Sornette, [Eur. Phys. J. B **2**, 525 \(1998\)](#).
- [39] A. Clauset, C. R. Shalizi, and M. E. J. Newman, [SIAM Rev. **51**, 661 \(2009\)](#).